JOURNAL OF MATERIALS SCIENCE 24 (1989) 4343–4349

Laser surface melting of low and medium carbon steels: influence on mechanical and electrochemical properties

J. M. PELLETIER, D. PERGUE, F. FOUQUET
GEMPPM, UA 341, BAT 502, INSA, 69621 Villeurbanne Cedex, France
H. MAZILLE
LPCI, BAT 401, INSA, 69621 Villeurbanne Cedex, France

The influence of a laser melting on both mechanical and electrochemical properties was studied in two carbon steels. Geometry and microstructure of the melt zone were first observed by optical and scanning electron microscopy, in various experimental conditions: with different interaction times and power density, for simple and multiple track melting. A large hardening was induced by the severe quenching resulting from rapid solidification; therefore the presence of hard points on the surface of the material may increase lifetime of specimens and improve tribological properties. This hardening created by the laser melting did not produce deleterious modifications of surface roughness or corrosion behaviour, at least in mildly corrosive saline solutions.

1. Introduction

Laser surface melting offers a means of achieving localized treatments; therefore surfaces with composite mechanical properties may be obtained and dimensions of treated zones may be varied over a wide range. From a metallurgical point of view, laser surface melting presents various advantages and opportunities: homogenization and dissolution of precipitated or segregated phases; rapid quenching from the melt leading to fine microstructure and consequently to possible improvement of mechanical properties.

There is considerable current interest in the use of laser melting in steels: stainless steels [1, 2], tool steels [3–5] or low carbon steels [6–10]. Several interesting features have been reported, especially about improvement in machining properties and lifetime in high-speed tool steels.

The present work was undertaken to study different aspects of laser melting in low and medium carbon steels: the influence of multiple track melting, especially on the heat-affected zone microstructure; the effect of laser treatment on corrosion resistance. Although such steels are not used for practical applications where good corrosion resistance is required, it is however interesting to observe the influence of microstructure changes on electrochemical properties. Indeed in some cases [11, 12], it has been reported that a microstructure refinement induced by a rapid solidification may improve the corrosion resistance.

Experiments were carried out using two kinds of laser: either a continuous-wave beam (CO_2) or a pulsed beam (YAG); a comparison of the two types of irradiation is made.

2. Experimental procedure

Two carbon steels were laser treated; their composition is given in Table I.

Specimens of parallelipiped shape ($50 \times 20 \times 8\,mm^3$) were mounted on a numerically controlled X–Y table and irradiated either with a continuous wave (CW) CO_2 laser (power up to 4 kW), or with a pulsed YAG laser (mean output power 300 W, pulse duration 0.2 to 20 m sec). Different treatment parameters were used to obtain various melt penetration depths; both single and multiple laser tracks are performed. No coating was used in order to avoid any contamination of the sample during melting. The surface oxidation was reduced by shielding the sample with an argon gas flow.

For optical and scanning electron microscopy, the samples were polished and etched in nital.

Composition analysis was performed by using secondary ion mass spectroscopy (SIMS); incident ions were oxygen ions.

Vickers microhardness measurements were taken with a load of 100 or 200 g. Some roughness determinations were also carried out.

For corrosion testing, the laser treated samples were cut into smaller specimens, and embedded in a cold curing resin, leaving an exposed area of about $12 \times 12\,mm^2$ for electrochemical investigations. An applied varnish at the alloy–epoxy interface prevented

TABLE I Composition (wt %) of the steels used

	C	S	Si	Mn	P	Cr	V
XC10	0.09	0.05	0.27	0.39	0.02	0.09	0.003
XC48	0.48	0.01	0.28	0.69	0.01	0.09	0.01

0022–2461/89 $03.00 + .12

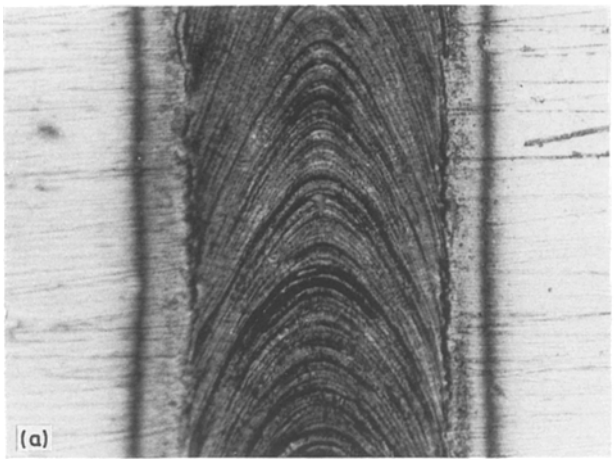

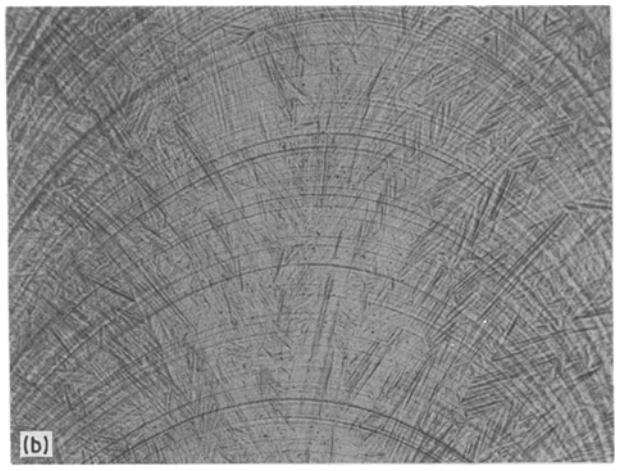

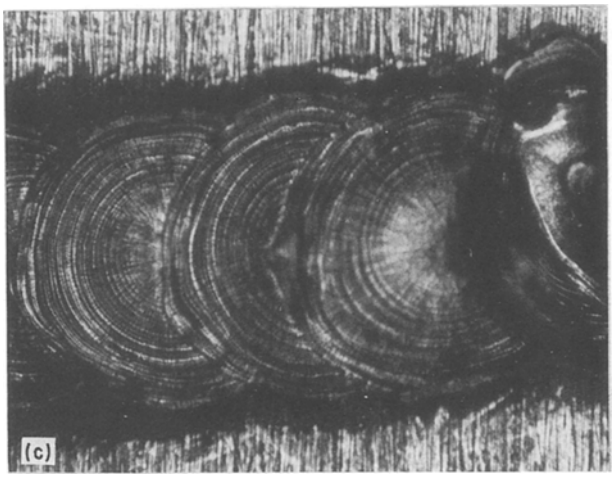

Figure 1 (a, b) Typical aspect of a laser melt surface; low carbon steel; $P = 800\,W$; defocusing distance 2 mm; $v = 1\,cm\,sec^{-1}$. (a) × 60; (b) × 200; (c) Solidification fronts due to surface melting produced by a pulsed laser; low carbon steel; $E = 2.2\,J$; $t = 1\,m\,sec$, × 100.

any leakage and any undesirable crevice effect or galvanic coupling with the copper wire welded on the back of the sample. Most of our experimental procedure concerning corrosion involved recording open-circuit potential with time of immersion and monitoring current–potential relationships using conventional potentiodynamic polarization techniques. The electrolyte (volume 500 cm^3) was a stirred Na_2SO_4 solution (0.1 $M\,l^{-1}$) at pH7 or 4 either aerated (open to the air) or deaerated by previous bubbling of pure argon. Potentiodynamic polarization curves were recorded (scan rate 1 $mV\,sec^{-1}$) with an EGG PAR model 273 potentiostat controlled by an external microcomputer. Polarization resistances, R_p, were calculated at open circuit potential ($I = 0$), from the polarization curves.

3. Results and discussion

3.1. Microstructural observations

3.1.1. Surface studies

A ripple structure is observed at all beam velocities and interaction times and periodicity is formed in solidification front spacing (Fig. 1). This phenomenon has been observed in different materials [13, 14]; its presence indicates that solidification is by no means uniform and stationary. The circular symmetry is clearly observed in pulsed-laser treated samples (Fig. 1b). Growth occurs along temperature gradients.

3.1.2 Microstructures

A longitudinal cross-section reveals the existence of three different zones (Fig. 2):

(i) the unaffected matrix – a classical low-carbon steel structure is observed, with two components, ferrite grains and pearlite;

(ii) the melted zone (MZ) – a highly distorted microstructure resulting from rapid solidification. Both optical and scanning electron microscopy reveal the existence of martensite in medium carbon steel; in the low carbon steel, acicular ferrite is present;

(iii) the heat affected zone (HAZ) – a large grain refining and a partial pearlite dissolution occurred through solid state transformation during the laser heating (Fig. 3). The resulting grain size is about 3 μm. Ashby and Easterling [7, 8] have studied this phenomenon in detail. As they have shown, the magnitude of these diffusional transformations depends on the number of atomic jumps made during the thermal cycle. The dissolution of pearlite requires carbon diffusion; assuming that the pearlite plate spacing is d, the colony may be converted into austenite if the lateral diffusion of carbon takes place over a distance d (or greater than d); this parameter is related to the diffusion coefficient and Ashby and Easterling [7] have shown that

$$d^2 = 2 D_0 \alpha \tau \exp(-Q/RT_p)$$

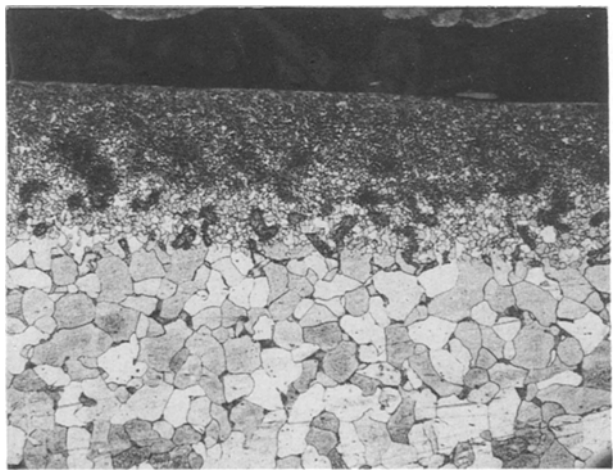

Figure 2 Optical micrograph of the heat-affected zone (upper part of the figure); low carbon steel; CO_2 laser; 800 W; 2 $cm\,sec^{-1}$, × 200.

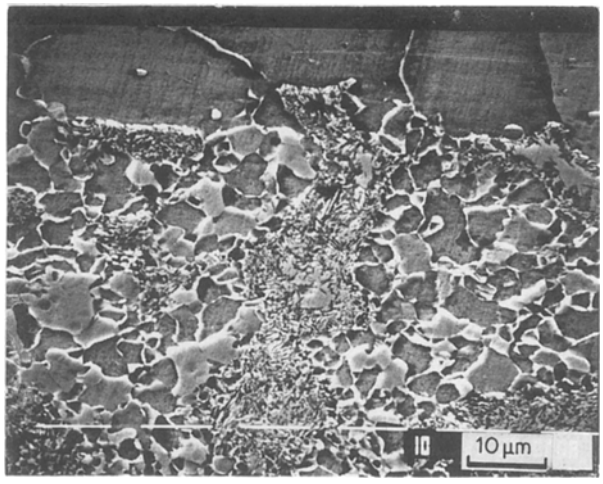

Figure 3 Scanning electron micrograph of the heat-affected zone; low carbon steel; YAG laser; 0.45 J; 0.2 m sec, × 1500.

where D_0 is the pre-exponential term for the diffusion coefficient, $\alpha = 3(RT_p/Q)^{1/2}$, T_p is the temperature required to induce the transformation, R is the gas constant and Q the activation energy for the transformation.

For insufficient duration of treatment, pearlite dissolution is incomplete, because carbon atoms diffuse over too short a distance, d. Furthermore, for the typical high heating rates of laser treatments, considerable superheatings of ferrite and pearlite are possible, thus also limiting the diffusion distances. Consequently, the partial diffusion of pearlite appears to be logical for the very short ageing times occurring for short laser-material interaction times.

An example of compositional SIMS analysis performed on cross-sections of samples (previously used for optical observations) is shown in Fig. 4. Carbon concentration (proportional to the observed intensity) has the same mean value for the whole sample: surface decarburizing does not occur during laser melting.

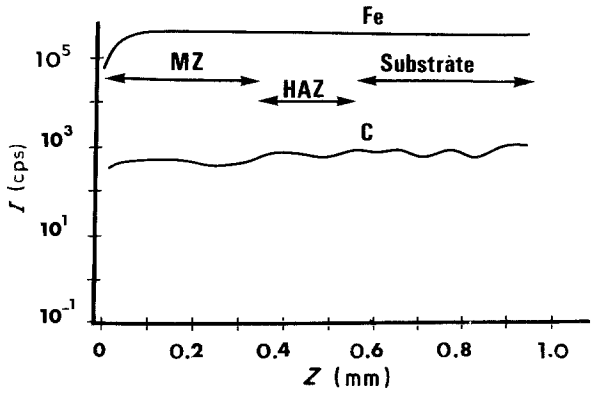

Figure 4 Carbon concentration plotted against depth; low carbon steel; CO_2 laser; 800 W; defocusing distance 2 mm; 1 cm sec^{-1}.

The three different zones (MZ, HAZ, matrix) may be distinguished: in the melt zone carbon concentration is homogeneous, confirming the existence of a fine microstructure and a uniform distribution of solute atoms in this zone. In the untreated material, the intensity variations indicate the alternance of ferritic and pearlitic zones.

3.1.3. Melt zone geometry

The melt geometry also depends strongly on the beam–material interaction time, t; for CW CO_2 treatments, t is simply related to the scanning speed, v ($t = \phi/v$, ϕ = laser beam diameter). For example, Fig. 5 shows the evolution of both width, W, and depth, D, of the melt zone as a function of v for a given power density; for high v values, a lenticular shape is observed, while for long treatment times (small v values), the classical keyhole phenomenon appears: D increases much more than W.

3.1.4. Influence of laser wavelength (λ)

Laser thermal treatments, and especially laser melting, are usually performed with CW CO_2 beams; a

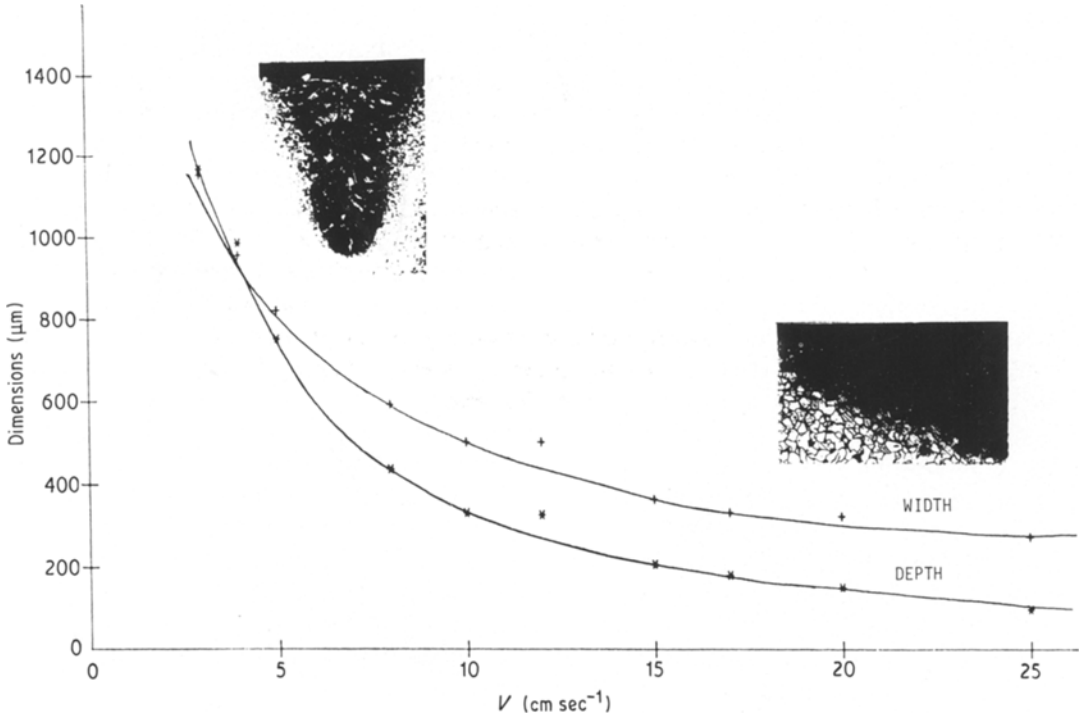

Figure 5 Geometry variation of the melt zone with the scanning rate; medium carbon steel; CO_2 laser; 700 W; defocusing distance 2 mm.

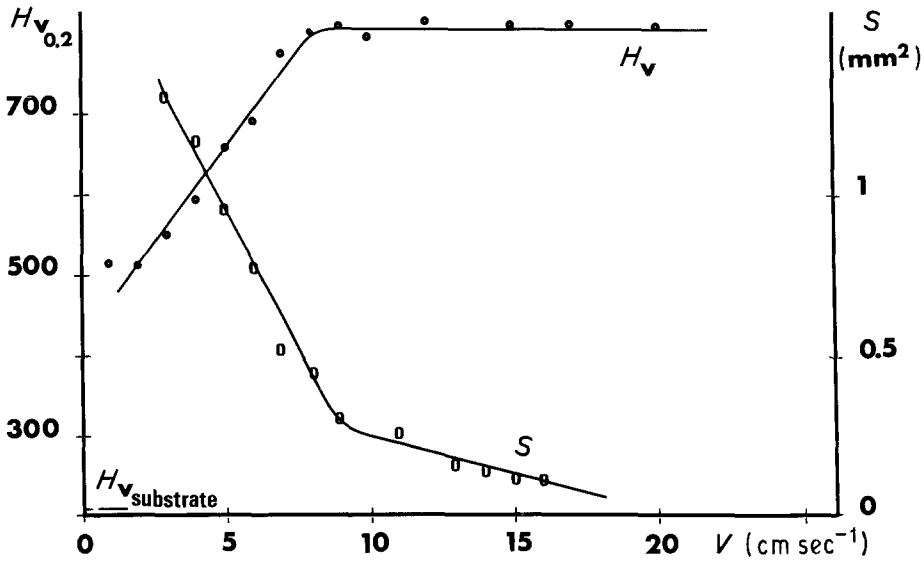

Figure 6 Variations of microhardness and surface of the melt zone with the scanning rate; medium carbon steel; CO_2 laser; 700 W.

comparison with results obtained with a pulsed laser, operating at a different wavelength, appears of interest. Therefore, some experiments were performed with a pulsed YAG apparatus. The absorption of the incident energy is better with this shorter wavelength (1.06 instead of 10.6 μm); therefore lower incident power density may be used. From a metallurgical point of view, no significant difference is observed: the same microstructures are revealed; martensite is formed in the melt zone and hardness values are similar (see section 3.2). The increase of cooling rate induced by the decrease of laser–material interaction time does not create any new metastable microstructure: only "classical" phases are observed in low or medium carbon steels.

Such treatments offer one advantage: very localized zones may be transformed (and then hardened); this is attractive from a technical point of view: the presence of hard points on the surface of the material may increase lifetime of specimens and improve tribological properties. However, such treatment using a pulsed laser give irregular surfaces, because large areas can be obtained only by addition of individual treated zones in both directions of the surface plane.

3.2. Influence on mechanical properties

3.2.1 Single track melting

First the influence of microstructural changes on hardness values was studied for single laser tracks, to avoid any "after-effect". The evolution of H_v as a function of depth, for a low carbon steel, is as follows: in the melted zone, H_v remains constant (about 400): this is due to the uniformity of microstructure and of carbon composition. This value is much larger than that of the substrate (about 160). A progressive decrease occurs in the heat-affected zone; in that zone the hardening may be attributed to the grain refining and, perhaps, to an increase of the carbon concentration in the ferrite.

In a medium carbon steel, a similar evolution is observed, but with higher hardness values, due to larger carbon content and to the existence of martensite. Average values are about 800 in the melted zone and 210 in the parent phase.

It is well known that quenching rate variations induce microstructural evolutions, especially in steels; this rate depends, for laser treatments in a given material, on two parameters: power density and interaction time, t, [15]; for a continuous wave laser beam, t is directly related to scanning rate v. Fig. 6 illustrates this effect on hardness value. The corresponding evolution of the surface of the melt zone (width × depth) is also reported. For $v = 8$ cm sec^{-1}, a transition occurs; for faster scanning rates hardness remains nearly constant, while for slower scanning rates an important hardness decrease is observed. A good correlation is obtained between hardness and surface S (i.e. also volume of the melt zone): the beginning of the hardness decrease corresponds to a rapid increase of S. The interpretation is as follows: as scanning speed decreases (dT/dt is roughly proportional to v) and for $v \leqslant 8$ cm sec^{-1}, the cooling rate is not sufficient to freeze the "out-of-equilibrium" state: carbon atoms can diffuse and initiate carbide precipitation; the microstructure moves progressively from a martensitic structure to a bainitic structure, as confirmed by micrograph observations. Therefore high hardness values cannot be obtained in deep laser melting treatments in low or medium carbon steels.

3.2.2. Multiple track melting

The obtention of large surface areas requires multiple track melting; therefore several successive meltings may occur for a given point of the sample, and solid state transformations may take place in regions previously melted (Fig. 7). The final aspect is shown schematically in Fig. 8; relative proportions of HAZ and MZ depends on laser treatment conditions: for given values of power density, P and scanning rate, v, the surface of the HAZ increases as the gap, d, between two passes decreases; for given values of P and d, the surface increases as v decreases, because the duration allowed for solid state transformation also increases. The consequence of these multiple treatments is shown in Fig. 9; hardness decrease

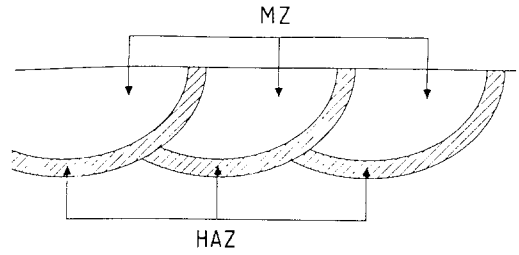

Figure 7 Schematic representation of a cross-section in the case of multiple track melting; the cross-hatched area corresponds to the heat-affected zone.

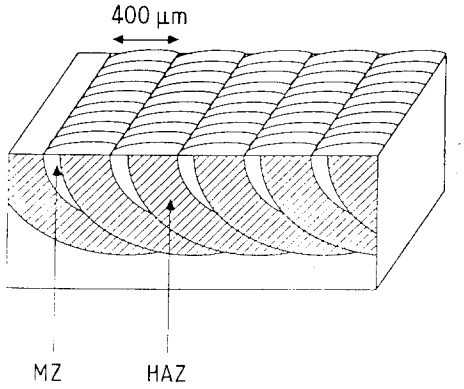

Figure 8 Relative areas of melt zone and heat-affected zone for two different multiple treatments.

results from the tempering effects induced by multiple scanning: the cycle heat treatment of previously laser-melted zones during successive tracks leads to the tempering of the martensite, as revealed by the optical microscopy. The microstructure is heterogeneous. In order to avoid this difficulty, it would be necessary to limit the carbon atom diffusion by decreasing the laser–material interaction time; but then the depth of treated zone would be very low, and this may be prejudicial for technological applications.

As previously mentioned, a "ripple structure" is observed at all beam velocities; however, a progressive change in the surface morphology occurs with increasing scanning velocity, v. As shown by our roughness measurements, the magnitude of ripples decreases as v increases. As suggested by Copley *et al.* [14], these ripples are created by a periodic overflow of liquid at the trailing edge of the molten pool; their reduction may well arise from attenuation in the shallow molten pool as scanning speed increases.

From a practical standpoint, it may be noticed that laser melting does not include a large roughness; indeed the magnitude of "surface waves" is no more than 1/100 mm.

3.3. Corrosion behaviour of surface-modified materials

The effect of surface modification through multi-track laser treatment on the corrosion properties of low carbon steels, was investigated for two different scanning rates, referred to as LST (low speed treatment: 2 cm sec^{-1}) and FST (fast speed treatment: 17 cm sec^{-1}). An untreated polished sample (0.25 μm diamond paste) was used as reference.

3.3.1 Corrosion behaviour in neutral solution

In deaerated neutral solution, the stabilized open-circuit potential of laser treated samples is slightly more noble than the untreated one (Fig.10), but the evolution of potentiodynamic polarization curves towards higher cathodic and anodic currents, indicates

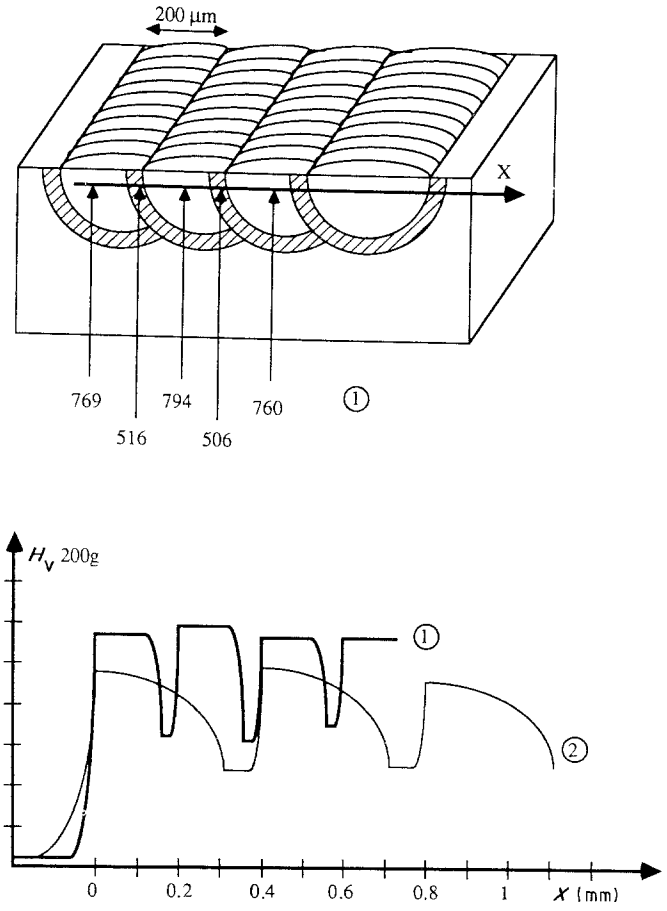

Figure 9 Microhardness measurements in a medium carbon steel (multiple treatment); CO_2 laser; defocusing distance 2 mm; P = 760 W. (1) v = 17 cm sec^{-1}, translation between two tracks = 200 μm; (2) v = 2 cm sec^{-1}, translation between two tracks = 400 μm.

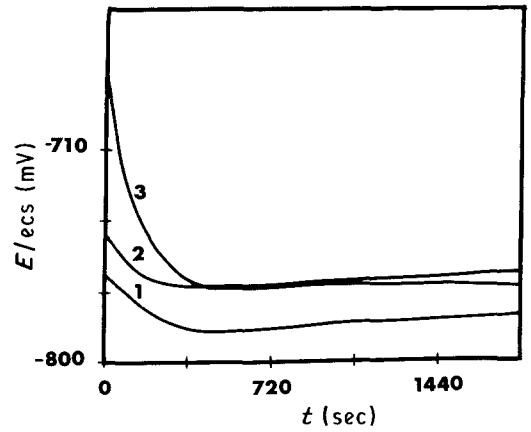

Figure 10 Open-circuit potential as a function of time, in a neutral solution, for various samples : (1) substrate; (2) LST; (3) FST.

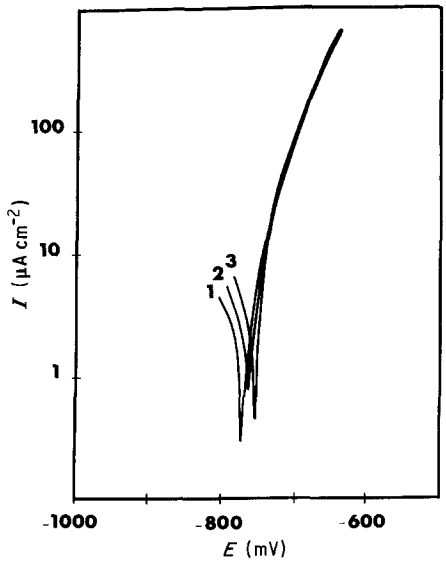

Figure 11 Potentiodynamic polarization curves in neutral solution; (1) substrate; (2) LST; (3) FST.

that laser treatment decreases the corrosion resistance of low-carbon steels (Fig. 11). This effect is more pronounced for the fast speed treatment, as confirmed by the computed data of current densities and corrosion rates from electrochemical measurements, reported in Table II. In such neutral solution, the corrosion rate is low and results mainly from the reduction of the remaining amounts of oxygen introduced during the sample immersion in the previously deaerated solution. The moderate decrease in corrosion behaviour with laser treatment may be due to increase in stressed areas or local defects (such as dislocations or vacancies) in the superficial melted layer, even if the laser treatment improves the chemical homogeneity as already stated (Fig. 4).

Such mechanical or structural defects enhance the reactivity of the surface towards the environment; but, more likely, the apparent increase in electrochemical reaction kinetics results from an enlargement of the actual surface of treated material in contact with the medium. In fact a multiplying coefficient of 1.6 to 1.8 (in order to take into account the "ripple structure" of the surface stressed above) is sufficient to explain the apparent modification of electrochemical behaviour.

We may conclude, therefore, in agreement with the observations of Peter *et al.* on steels under the same experimental conditions [16, 17], that laser treatment has no significant or deleterious influence on the corrosion behaviour of mild steels in aqueous neutral solution.

3.3.2 Corrosion behaviour in mildly acid aqueous solution

The addition of sulphuric acid to Na_2SO_4 solution does not change the open-circuit potential of laser-treated samples greatly compared to untreated ones, at least up to pH4. On the other hand, in such conditions, this increase in corrosion rates, as reported in Table III, cannot be explained by enlargement of the reactive surface due to the "ripple-effect".

At pH4 the main cathodic reaction controlling the overall corrosion process is hydrogen evolution, and it is well known [18] that the kinetics of such a reaction is not only strongly dependent on the pH of the solution, but also on alloy composition and structure such as amounts of impurities or segregations, nature of precipitates. Laser treatments lead, in acidified solutions, to an unfavourable metallurgic structure, at least from a corrosion standpoint.

We must point out that in both types of solution (neutral or acidified) we observe only uniform attack, without any localized effect such as pitting or crevices. That behaviour is also confirmed by polarization curve recordings, which are very similar whatever the voltage scanning direction (forward to more noble potential or reverse).

4. Conclusion

By laser melting, surfaces with composite mechanical properties may be obtained. The melt zone geometry depends mainly on parameters used for treatments, especially power density and interaction time; large variations of both width and depth are easily realized.

The melting, followed by a rapid solidification, may induce an attractive hardening of the surface; for instance, Vicker's hardness values of 400 and 800 are obtained for low and medium carbon steels,

TABLE II Electrochemical determination of corrosion rates of low carbon steel (0.1 wt %) in deaerated neutral Na_2SO_4 solution (0.1 Ml^{-1})

	Material		
	Untreated sample	Low-speed treatment	Fast-speed treatment
i_{cor} ($\mu A\,cm^{-2}$)	4.14	6.7	7.5
e ($\mu m\,yr^{-1}$)	49	79	88

TABLE III Electrochemical determinations on low carbon steels in acidified Na_2SO_4 solution (pH4).

	Material		
	Untreated sample	Low-speed treatment	Fast-speed treatment
R_p ($K\,cm^2$)	1.68	0.24	0.24
i_{cor} ($\mu A\,cm^{-2}$)	13	93	93
e ($\mu m\,y^{-1}$)	152	1090	1090

respectively. This is due to the formation of a fine-grain martensite; high hardness values are also produced by solid state transformation in the heat-affected zone; micrographic observations reveal a large grain refinement in this zone.

However two problems occur:

(i) too slow treatments, producing a deep melt zone, must be avoided, because the decrease of quenching rate induces the formation of a bainitic structure (instead of a martensitic structure) and then a decrease of the hardening effect;

(ii) multiple track melting induces a tempering of the martensite obtained in previously laser-melted zones; the microstructure observed on a cross-section indicates a heterogeneous aspect and softening effects are related to this tempering.

Therefore, single pass treatment appears more attractive, and then the difficulty is to realize adequate areas of treated material to produce an enhancement of the local desired properties, e.g. wear resistance.

Finally it may be noticed that laser melting of low or medium carbon steels does not produce critical modifications of surface roughness, or corrosion behaviour, at least in mildly corrosive saline solutions.

References

1. N. WADE, T. KOSHIHAMA and Y. HOSOI, *Scripta Metall.* **19** (1985) 859.
2. P. A. MOLIAN and W. E. WOOD, *J. Mater. Sci.* **18** (1983) 2555.
3. P. R. STRUTT, H. NOVOTNY, M. TULI and B. H. KEAR, *Mater. Sci. Engng* **36** (1978) 217.
4. P. R. STRUTT, *ibid.* **44** (1980) 239.
5. G. BARTON, M. DIEFENBACH and J. BETZ, Proceedings of the Conference on "Rapidly Quenched Metals", edited by S. Steeb and H. Warlimont (Elsevier Science, Amsterdam, 1985) p. 855.
6. M. CARBUCICCHIO, G. MEAZZA, G. PALOMBARINI and G. SABOGNA, *J. Mater. Sci.* **18** (1983) 1543.
7. M. F. ASHBY and K. E. EASTERLING, *Acta Metall.* **32** (1984) 1935.
8. *Idem, ibid.* **34** (1986) 1533.
9. M. CARBUCICCHIO and G. PALOMBARINI, *J. Mater. Sci.* **21** (1986) 75.
10. P. CANOVA and E. RAMOUS, *ibid.* **21** (1986) 2143.
11. T. R. ANTHONY and H. E. CLINE, *J. Appl. Phys.* **49** (1978) 1248.
12. E. McCAFFERTY, P. G. MOORE and G. T. PEACE, *J. Electrochem. Soc.* **129** (1982) 9.
13. T. R. ANTHONY and H. E. CLINE, *J. Appl. Phys.* **48** (1977) 3888.
14. S. M. COPLEY, D. BECK, O. ESQUIVEL and M. BASS, in "Laser-Solid Interactions and Laser Processings", edited by S. D. Ferris, H. J. Leamy and J. M. Poate, American Institute Conference Proceedings, New York, 50 (1979) p. 161.
15. H. S. CARSLAW and J. C. JAEGER, in "Conduction of Heat in Solids", (Clarendon, Oxford, 1959).
16. R. PETER, W. LÖSCHAU, W. POMPE and W. FORKER, *Werkstoffe und Korrosion* **37** (1986) 621.
17. R. PETER, K. E. EICHHORN and W. FORKER, *Z. Phys. Chem. Leipzig* **256** (1987) 1169.
18. H. H. UHLIG, "Corrosion and Corrosion Control", 2nd Edn (Wiley, New York, 1985).

Received 16 September 1988
and accepted 24 February 1989